Local defects and ferromagnetism in graphene layers

M. A. H. Vozmediano,[1] M. P. López-Sancho,[2] T. Stauber,[2] and F. Guinea[2,3]
[1]*Unidad Asociada CSIC-UC3M, Universidad Carlos III de Madrid, E-28911 Leganés, Madrid, Spain*
[2]*Instituto de Ciencia de Materiales de Madrid, CSIC, Cantoblanco, E-28049 Madrid, Spain*
[3]*Department of Physics, Boston University, 590 Commonwealth Avenue, Boston, Massachusetts 02215, USA*
(Received 29 June 2005; revised manuscript received 30 August 2005; published 28 October 2005)

We study the changes in the electronic structure induced by lattice defects in graphene planes. In many cases, lattice distortions give rise to localized states at the Fermi level. Electron-electron interactions lead to the existence of local moments. The RKKY interaction between these moments is always ferromagnetic, due to the semimetallic properties of graphene.

DOI: 10.1103/PhysRevB.72.155121 PACS number(s): 75.10.Jm, 75.10.Lp, 75.30.Ds

I. INTRODUCTION

A number of recent experiments suggest that pure graphite behaves as a highly correlated electron system.[1] In particular, it shows a metal-insulator transition in magnetic fields and insulating behavior in the direction perpendicular to the planes in different samples.[1–8] Recent results show ferromagnetic behavior,[9] enhanced by proton bombardment,[10] which opens up a new way to the creation of organic magnets.[11] In this paper we study the formation of local moments near extended defects. It is shown that many types of lattice distortions, like cracks and large voids, can induce localized states at the Fermi level, leading to the existence of local moments. The RKKY interaction between these moments is always ferromagnetic due to the semimetallic properties of graphite. Hence, the RKKY interaction does not lead to frustration and spin glass features.

We outline the model to be studied in the next section. In Sec. III we present analytical and numerical calculations that show the possibility of localized electronic states near extended defects. In the next section we analyze the formation of local moments associated with these states, due to a local repulsive electron-electron interaction. Then, we discuss the nature of the coupling between these local moments and the bulk magnetic properties that they can induce. Section VI contains the main conclusions of our work.

II. THE MODEL

The conduction band of graphite is well described by a tight binding model that includes the π orbitals that are perpendicular to the graphite planes at each C atom.[12] If the interplane hopping is neglected, this model describes a semimetal, with a zero density of states at the Fermi energy, and where the Fermi surface is reduced to two inequivalent K points located at the corner of the hexagonal Brillouin zone. If we only keep nearest neighbor hopping terms, the electronic bands are described by the tight-binding Hamiltonian:

$$\mathcal{H}_{\mathrm{TB}} = t \sum_{i,jn.n.;s} c^{\dagger}_{i,s} c_{j,s} + \mathrm{H.c.}, \tag{1}$$

where $t \sim 2.7$ eV. The corresponding dispersion relation of the two π bands is

$$\epsilon_{\mathbf{k}} = \pm 3t \sqrt{\cos(\mathbf{k}\mathbf{a}_1) + \cos(\mathbf{k}\mathbf{a}_2) + \cos[\mathbf{k}(\mathbf{a}_1 - \mathbf{a}_2)]}, \tag{2}$$

where $\mathbf{a}_1$ and $\mathbf{a}_2$ are the unit vectors of the honeycomb lattice.

The low-energy excitations with momenta in the vicinity of the Fermi points have a linear dispersion and can be described by a continuum model that reduces to the Dirac equation in two dimensions.[12–16] The Hamiltonian density of the system is

$$\mathcal{H}_0 = \hbar v_{\mathrm{F}} \int d^2\mathbf{r}\, \bar{\Psi}(\mathbf{r})(i\sigma_x \partial_x + i\sigma_y \partial_y)\Psi(\mathbf{r}), \tag{3}$$

where σ_i are the Pauli matrices, $v_{\mathrm{F}} = (3ta)/2$, and $a = 1.4$ Å is the distance between nearest carbon atoms. The components of the two-dimensional spinor,

$$\Psi(\mathbf{r}) = \begin{pmatrix} \Psi_1(\mathbf{r}) \\ \Psi_2(\mathbf{r}) \end{pmatrix}, \tag{4}$$

correspond to the amplitude of the wave function in each of the two sublattices that build up the honeycomb structure. They satisfy the equation

$$(i\partial_x \pm \partial_y)\Psi_1(\mathbf{r}) = \epsilon \Psi_2(\mathbf{r}),$$

$$(i\partial_x \mp \partial_y)\Psi_2(\mathbf{r}) = \epsilon \Psi_1(\mathbf{r}), \tag{5}$$

where the two signs on the right-hand side correspond to the two inequivalent corners of the Brillouin zone.

In the clean two-dimensional system there is no room for low-energy electronic instabilities, as the short-range interactions are made irrelevant in the renormalization group sense by the vanishing density of states at the Fermi level.

III. BOUND STATES NEAR CRACKS AND OTHER LATTICE DEFECTS

A. Continuum approximation

It is known that disorder significantly changes the states described by the two-dimensional Dirac equation,[17–19] and, usually, the density of states at low energies is increased. Lattice defects, such as pentagons and heptagons, or dislocations, can be included in the continuum model by means of a

non-Abelian gauge field[14,20] that reproduces the effects of the curvature of the lattice and the possible exchange of Fermi points. Within the same theoretical scheme it has also been shown that certain types of disorder randomly distributed in the graphene lattice enhances the effect of the interactions[21] and can stabilize new phases. In addition, a graphene plane can show states localized at interfaces,[22,23] which, in the absence of other types of disorder, lie at the Fermi energy. Structures with mixed sp^2 and sp^3 bonding can also lead to localized states.[24]

The tight-binding model defined by the π orbitals at the lattice sites can have edge states when the sites at the edge belong all to the same sublattice[22,23,25] (zigzag edge). These states lie at zero energy which for neutral graphene planes correspond to the Fermi energy. In the continuum model described earlier, these localized states are normalizable solutions $[\Psi_1(\mathbf{r}),\Psi_2(\mathbf{r})]$ of the Dirac equation, Eq. (5) for $\epsilon=0$,

$$(i\partial_x \pm \partial_y)\Psi_1(\mathbf{r}) = i\partial_{z,\bar{z}}\Psi_1(z,\bar{z}) = 0,$$

$$(i\partial_x \mp i\partial_y)\Psi_2(\mathbf{r}) = i\partial_{\bar{z},z}\Psi_2(z,\bar{z}) = 0, \tag{6}$$

where $z,\bar{z}=x\pm iy$. These equations are satisfied if $\Psi_1(\mathbf{r})$ is an analytic function of z and $\Psi_2(\mathbf{r})=0$, or if $\Psi_1(\mathbf{r})=0$ and $\Psi_2(\mathbf{r})$ is an analytic function of $\bar{z}$.

We now consider a semi-infinite honeycomb lattice with an edge at $y=0$ and that occupies the half-plane $x>0$. A possible solution that decays as $x\to\infty$ is

$$\Psi_1(x,y) \propto e^{-kz} = e^{iky}e^{-kx}, \quad \Psi_2(\mathbf{r}) = 0.$$

These solutions satisfy the boundary conditions at $y=0$ if the last column of carbon atoms belong to the sublattice where the component Ψ_1 is defined. Then, the next column belongs to the other sublattice, where the amplitude of the state is, by construction, zero.

These kinds of solutions can be generalized to describe other types of extended defects that will be produced in experiments where graphite samples are bombarded by protons. In a strongly disordered sample, large defects made up of many vacancies can exist. These defects will give rise to localized states, when the termination at the edges is locally similar to the surfaces discussed above. Note that if the bonds at the edges are saturated by bonding to other elements, like hydrogen, the states at these sites are removed from the Fermi energy, but a similar boundary problem arises for the remaining π orbitals. The only possible localized states can exist at zero energy, where the density of extended states vanishes. The wave functions obtained from the Dirac equations will be normalizable and analytic functions of the variables $z=x+iy$ or $\bar{z}=x-iy$ of the form,

$$\Psi(z) \equiv [f(z),0]$$

obeying the boundary conditions imposed by the shape of the defect.

Extended vacancies with an approximate circular shape can support solutions of the type

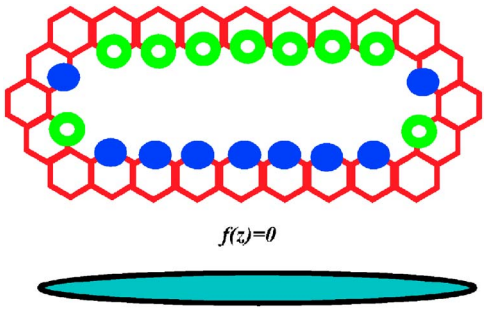

FIG. 1. (Color online) Elongated crack in the honeycomb structure. The crack is such that the sites in the upper edge belong to one sublattice, while those at the lower edge belong to the other. Bottom: an approximate cut in the complex plane that can be used to represent this crack at long distances.

$$f(z) \propto z^{-n}, \quad n > 1.$$

By using conformal mapping techniques, solutions can be found with the boundary conditions appropriate to the shapes of different defects.

A simple case is the elongated crack depicted in Fig. 1, which we assume to extend from $x=-a$ to $x=a$, and to have a width comparable to the lattice constant along the y axis. The analytic function $f(z)$ associated with localized states near a crack of this shape should satisfy $\mathrm{Re}\, f(z)=0$ at the crack edges, because the boundaries of the crack include atoms from the two sublattices. Hence, the boundary of the crack leads to a branch cut in the complex function $f(z)$. Labeling edge states by a quantum number n, we find that the function Ψ can be written for these states as

$$\Psi_n \equiv \left[\mathrm{Re}\left(\frac{A}{z^n\sqrt{z^2-a^2}}\right),0\right].$$

A similar solution is obtained by exchanging the upper by the lower spinor component, and replacing $z\leftrightarrow\bar{z}$. Because of the discreteness of the lattice, the allowed values of n should be smaller than the number of lattice units spanned by the crack.

B. Lattice model

We have checked numerically the existence of these localized states by diagonalizing the tight-binding Hamiltonian in finite lattices of different sizes. The dependence of some of the states close to the chemical potential (zero energy) on the cluster size is shown in Fig. 2. The delocalized states show a dependence $\epsilon_{\mathrm{del}} \propto L^{-1}$, consistent with the properties of the Dirac equation from which they can be derived. The states closest to $\epsilon=0$ show a dependence $\epsilon_{\mathrm{loc}} \propto L^{-2}$, which suggest a power law localization, in agreement with the previous analysis. The total density of states of a given cluster is shown in Fig. 3.

These states are half-filled in a neutral graphene plane. In the absence of electron interactions, this leads to a large degeneracy in the ground state.

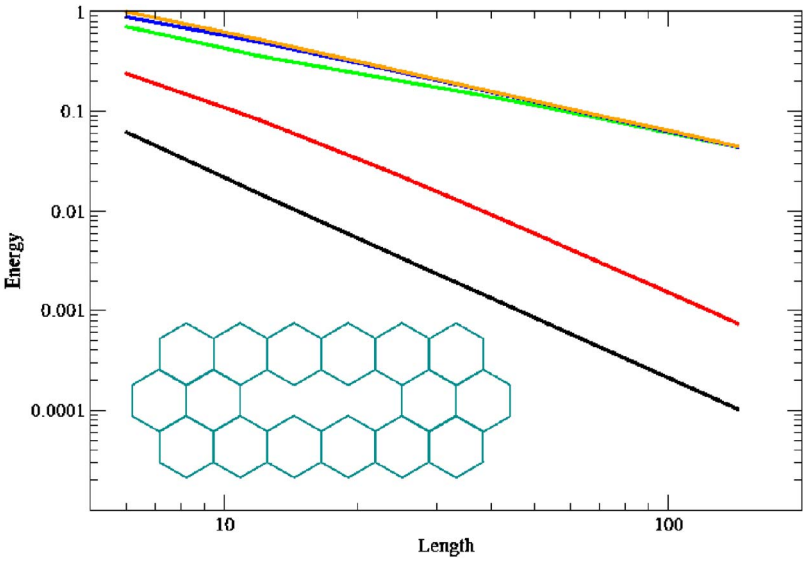

FIG. 2. (Color online) Energy of the five states with positive energy closest to $\epsilon=0$ for a cluster of size $L\times L$ that contains at the center the defect shown in the inset. Periodic boundary conditions are used. The spectrum is symmetric around $\epsilon=0$.

IV. ELECTRON ELECTRON INTERACTIONS

In the presence of a finite local repulsion, the flat band of localized states will tend to become polarized, leading to a a ferromagnetic alignment of the electrons occupying these states, as in similar cases with degenerate bands.[26] This effect has been found numerically for the surface states near flat edges discussed previously.[27,28]

We have checked the formation of local moments near cracks and similar defects by performing Hartree-Fock calculations in finite clusters, and modeling the electron-electron interaction by an on site repulsive term U. A typical total density of states for the unpolarized state of a cluster with 24×24 unit cells and a large defect as the one shown in Fig. 1 are shown in Fig. 3. A small, but finite repulsive, term, $U=0.5t\simeq 1.4$ eV, leads to the splitting of a central peak, as shown in Fig. 4. The total polarization of the cluster is also small. Similar results are obtained with an arbitrary number of contiguous vacancies. In all cases the total polarization of the cluster is proportional to the excess of sites of one sublattice over the other in the edge n_A-n_B, which agrees with previous results[29] and shows that only the electrons from the states around the impurity contribute to the formation of a local moment.

This calculation assumes that the Fermi level is pinned at $\epsilon_F=0$, and that the electronic spectrum shows electron hole symmetry around this energy. A finite doping, like that induced by an external gate used in Ref. 30, leads to a finite Fermi energy, and ϵ_F will reduce the tendency toward the formation of a local moment. A similar effect can be expected from hopping terms between sites in the same lattice, t', which break electron-hole symmetry,[31] which will tend to broaden the localized state discussed here. The previous analysis, however, remains qualitatively valid, provided that $\epsilon_F, t' \ll U$.

V. COUPLING BETWEEN LOCAL MOMENTS

A. RKKY interaction

We have shown in the previous section that large lattice defects induce localized electronic states in their vicinity,

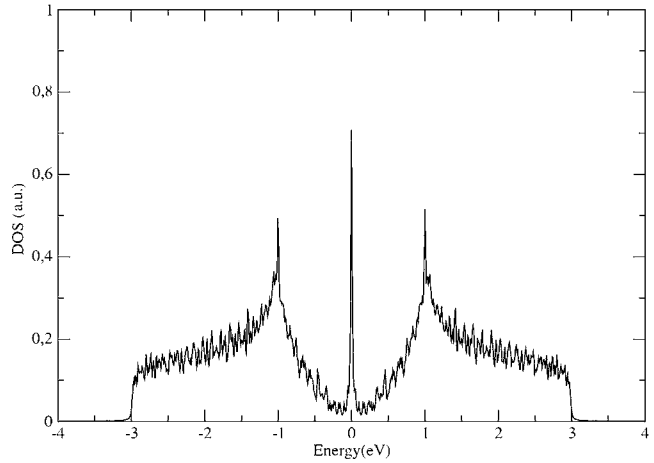

FIG. 3. Density of states of a 24×24 cluster with a large defect as the one shown in Fig. 1. The on-site interaction term is $U=0$.

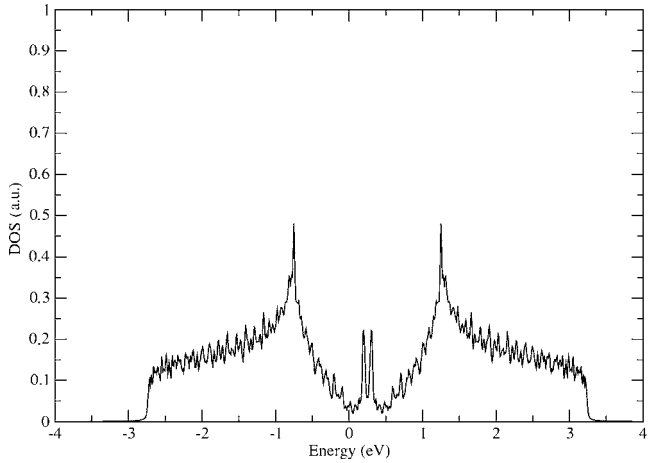

FIG. 4. The same as Fig. 3 with an on-site interaction $U=0.5t$.

which, in turn, lead to the formation of local moments. These local moments interact with the extended states, which will mediate a RKKY-like interaction between local moments at neighboring defects. A spin polarized electron in a localized state $|\Psi_m\rangle$ gives rise to an effective magnetic field at each site of order $m \sim U|a_{ij}^m|^2$, where a_{ij}^m is the amplitude of state m at site ij. This field favors the occupancy of that site with electrons in extended states with the same spin as that of the localized electrons (note that typically the exchange interaction between electrons at different sites is antiferromagnetic). The change in the wave function of the extended electrons can be calculated using perturbation theory, in terms of the spin susceptibility of a clean system. The susceptibility per unit area was calculated in Ref. 16, and can be written, at small momenta, as

$$\chi(\mathbf{q}) \propto \frac{|\mathbf{q}|}{v_{\mathrm{F}}}. \tag{7}$$

The total potential induced around a defect is

$$m \sim U \sum_{m;ij} |a_{ij}^m|^2 \sim NU, \tag{8}$$

where $N \sim L_d/a$, L_d is proportional to the length of the perimeter of the defect, and a is the carbon-carbon distance. This potential is distributed over an area comparable, or larger to, the surface of the defect, $A_d \sim L_d^2$. Combining Eq. (7) and Eq. (8), we obtain

$$J_{RKKY}(\mathbf{r}) \sim U^2 N_d^2 a^4 \int_{|\mathbf{k}| \ll L_d^{-1}} d^2\mathbf{k}\, e^{i\mathbf{kr}} \frac{|\mathbf{k}|}{v_{\mathrm{F}}} \sim U^2 N_d^2 \frac{a^4}{v_F |\mathbf{r}|^3}, \tag{9}$$

where a is the lattice constant.

Due to the absence of a finite Fermi surface, the RKKY interaction in Eq. (9) does not have oscillations. Hence, there are no competing ferro- and antiferromagnetic couplings, and the magnetic moments will tend to be ferromagnetically aligned. The total polarization per unit area at low temperatures is proportional to $c \times N_d$, where c is the concentration of defects, and N_d is proportional to their average size.

B. Collective effects. Ferromagnetism

We can make an estimate of the Curie temperature from the coupling between the local magnetic moments given in Eq. (9). The entropy cost of aligning ferromagnetically moments is $S \sim T$ per moment. The average distance between moments is $|\mathbf{r}| \sim c^{-1/2}$. Hence, the free energy per moment in the ferromagnetic phase can be written as

$$\mathcal{F}(m) = \left(- c_1 \frac{U^2 N_d^2 a^4 c^{3/2}}{v_{\mathrm{F}}} + c_2 T \right) m^2 + \cdots, \tag{10}$$

where c_1 and c_2 are numerical constants of order unity. The value of the free energy will be negative (and below the value in the paramagnetic phase) at a Curie temperature, given by

$$T_c \sim \frac{U^2 N_d^2 a^4 c^{3/2}}{v_{\mathrm{F}}} \approx \frac{U^2}{W} \frac{N_d a^3}{l^3}, \tag{11}$$

where W is the conduction electron bandwidth, $W \sim v_{\mathrm{F}}/a \sim t$, and l is the average distance between impurities.

The Curie temperature depends on the concentration and size of the defects. Assuming, as an example, that $N_d \sim 10$ and $l \sim 10^2 a$, we obtain a saturation magnetization of 10^{-3} Bohr magnetons per unit cell, and a Curie temparature $T_{\mathrm{C}} \sim 10^{-4} U^2/W$. The value of U^2/W can be estimated to be ~ 1 eV. Then, these arguments give $T_C \sim 1$ K. This temperature is considerably lower than the experimentally observed ones. It is worth noting, however, that this analysis does not take into account the enhancement of the susceptibility of the conduction electrons, percolation effects due to the random distribution of impurities, and the finite extension of the localized states induced by the defects.

This analysis does not take into account the effects of a shift in the Fermi energy, ϵ_{F}, due to doping. In a doped graphene sheet, a finite Fermi momentum, $k_{\mathrm{F}} = \epsilon_{\mathrm{F}}/v_{\mathrm{F}}$ will lead to oscillations with wavelength $2k_{\mathrm{F}}$ superimposed to the interaction described in Eq. (9). These oscillations lead to competing ferro- and antiferromagnetic couplings at distances greater than $k_{\mathrm{F}}^{-1} \propto n^{-1/2}$, where n is the concentration of carriers. If the distance between defects is smaller than this value, the RKKY interaction remains ferromagnetic, and the conclusions of this section are valid. Note, in addition, that defects tend to suppress the sharpness of the Fermi surface.

VI. CONCLUSIONS

We have shown that, under very general circumstances, lattice defects, vacancies, and voids in the graphene structure give rise to localized states at the Fermi energy. The number of these states scales roughly with the perimeter of the defect. Repulsive electron-electron interactions lead to the polarization of these states, and to the formation of local moments. The RKKY interaction mediated by the valence electrons decays as r^{-3}, where r is the distance between defects, and shows no oscillations, due to the vanishing of the Fermi surface in a graphene layer. The interaction is ferromagnetic, and the system cannot show the frustration effects and spin glass features observed in other disordered systems with local moments. On the other hand, the Curie temperature estimated assuming a random distribution of local moments is low, $T_{\mathrm{C}} \sim 1$ K, for reasonable values of the defect concentration. It may happen that percolation effects, and the finite extension of the localized states that give rise to the local moments will increase the value of T_{C}.

ACKNOWLEDGMENTS

We thank P. Esquinazi for sharing his experiments with us and for many illuminating discussions. Funding from MCyT (Spain) through Grant No. MAT2002-0495-C02-01 is acknowledged. One of us (F.G.) would like to thank Boston University for their hospitality, where part of this work was done.

[1] Y. Kopelevich, P. Esquinazi, J. H. S. Torres, R. R. da Silva, and H. Kempa, in *Studies of High Temperature Superconductors*, edited by A. Narlikar (Nova Science, New York, 2003), Vol. 45, p. 59.
[2] Y. Kopelevich, P. Esquinazi, J. H. S. Torres, and S. Moehlecke, J. Low Temp. Phys. **119**, 691 (2000).
[3] P. Esquinazi, A. Setzer, R. Höhne, C. Semmelhack, Y. Kopelevich, D. Spemann, T. Butz, B. Kohlstrunk, and M. Lösche, Phys. Rev. B **66**, 024429 (2002).
[4] H. Kempa, P. Esquinazi, and Y. Kopelevich, Phys. Rev. B **65**, 241101(R) (2002).
[5] S. Moehlecke, P.-C. Ho, and M. B. Maple, Philos. Mag. B **82**, 1335 (2002).
[6] J. M. D. Coey, M. Venkatesan, C. B. Fitzgerald, A. P. Douvalis, and I. S. Sanders, Nature **420**, 156 (2002).
[7] Y. Kopelevich, J. H. S. Torres, R. R. da Silva, F. Mrowka, H. Kempa, and P. Esquinazi, Phys. Rev. Lett. **90**, 156402 (2003).
[8] H. Kempa, H. C. Semmelhack, P. Esquinazi, and Y. Kopelevich, Solid State Commun. **125**, 1 (2003).
[9] K. h. Han, D. Spemann, P. Esquinazi, R. Höhne, R. Riede, and T. Butz, Adv. Mater. (Weinheim, Ger.) **15** (20), 1719 (2003).
[10] P. Esquinazi, D. Spemann, R. Höhne, A. Setzer, K.-H. Han, and T. Butz, Phys. Rev. Lett. **91**, 227201 (2003).
[11] T. L. Makarova, in *Studies of High-T_c Superconductivity*, edited by A. Narlikar (Nova Science, New York, 2003).
[12] J. C. Slonczewski and P. R. Weiss, Phys. Rev. **109**, 272 (1958).
[13] J. W. McClure, Phys. Rev. **112**, 715 (1958).
[14] J. González, F. Guinea, and M. A. H. Vozmediano, Nucl. Phys. B **406**, 771 (1993).
[15] J. González, F. Guinea, and M. A. H. Vozmediano, Nucl. Phys. B **424**, 595 (1994).
[16] J. González, F. Guinea, and M. A. H. Vozmediano, Phys. Rev. Lett. **77**, 3589 (1996).
[17] C. de C. Chamon, C. Mudry, and X.-G. Wen, Phys. Rev. B **53**, R7638 (1996).
[18] H. E. Castillo, C. C. Chamon, E. Fradkin, P. M. Goldbart, and C. Mudry, Phys. Rev. B **56**, 10668 (1997).
[19] B. Horovitz and P. La Doussal, Phys. Rev. B **65**, 125323 (2002).
[20] J. González, F. Guinea, and M. A. H. Vozmediano, Phys. Rev. B **63**, 134421 (2001).
[21] T. Stauber, F. Guinea, and M. A. H. Vozmediano, Phys. Rev. B **71**, 041406(R) (2005).
[22] K. Wakabayashi and M. Sigrist, Phys. Rev. Lett. **84**, 3390 (2000).
[23] K. Wakabayashi, Phys. Rev. B **64**, 125428 (2001).
[24] A. A. Ovchinnikov and I. L. Shamovsky, J. Mol. Struct.: THEOCHEM **251**, 133 (1991).
[25] K. Harigaya, A. Yamashiro, Y. Shimoi, K. Wakabayashi, Y. Kobayashi, N. Kawatsu, K. Takai, H. Sato, J. Ravier, T. Enoki, and M. Endo, J. Phys. Chem. Solids **65**, 123 (2004).
[26] D. Vollhardt, N. Blümer, K. Held, M. Kollar, J. Schlipf, M. Ulmke, and J. Wahle, Adv. Solid State Phys. **38**, 383 (1999).
[27] A. Yamashiro, Y. Shimoi, K. Harigaya, and K. Wakabayashi, Physica E (Amsterdam) **22**, 688 (2004).
[28] A. Yamashiro, Y. Shimoi, K. Harigaya, and K. Wakabayashi, Phys. Rev. B **68**, 193410 (2003).
[29] K. Kusakabe and M. Maruyama, Phys. Rev. B **67**, 092406 (2003).
[30] K. S. Novoselov, A. K. Geim, S. V. Morozov, D. Jiang, Y. Zhang, S. V. Dubonos, I. V. Gregorieva, and A. A. Firsov, Science **306**, 666 (2004).
[31] N. M. R. Peres, F. Guinea, and A. H. C. Neto, 2005, cond-mat/0506709 (unpublished).